

WAVE RUN-UP AND WAVE OVERTOPPING UNDER VERY OBLIQUE WAVE ATTACK (CORNERDIKE-PROJECT)

Antje Bornschein (1), Reinhard Pohl (1), Vincent Wolf (1), Holger Schüttrumpf (2),
Babette Scheres (2), Peter Troch (3), Jaromar Riha (4), Jentsje W. van der Meer (5)

- (1) TU Dresden, Germany, E-mail: antje.bornschein@tu-dresden.de
 (2) RWTH Aachen University, Germany, E-mail: schuettrumpf@iww.rwth-aachen.de
 (3) Ghent University, Belgium, E-mail: Peter.Troch@UGent.be
 (4) Brno University of Technology, Czech Republic, E-mail: riha.j@fce.vutbr.cz
 (5) VanderMeer Consulting B.V., Netherlands, E-mail: jm@vandermeerconsulting.nl

Within the CornerDike project (HyIV-DHI-05) wave run-up and wave overtopping under very oblique wave approach was investigated. The following paper describes the model set-up and measurement instrumentation in the shallow water basin at the Danish Hydraulic Institute at Hørsholm, Denmark where the tests were made. The short result analysis focuses on long crested wave although the model tests included short crested waves as well. But for the latter the result analysis is still in progress.

1. INTRODUCTION

A reliable calculation of the wave run-up on slopes is needed for the freeboard design at levees and embankment dams as well as for the recalculation or analysis of observed events. Wave overtopping is significant in risk assessment for coastal protection structures. Wave run-up and wave overtopping are influenced by dike characteristics as well as wave characteristics. An oblique wave attack lessens in general the wave run-up height and the wave overtopping volume. Several former investigations aimed at quantifying the influence of oblique wave approach. Especially in the range of very oblique wave approach with angles beyond 60 degree only few data are available. The hydraulic model tests of the CornerDike-project tried to fill this gap.

2. FORMER INVESTIGATIONS

The EUROTROP-Manual (EurOtop, 2007) recommends the following formulae for calculation of wave run-up $R_{u2\%}$ which is only exceeded by 2 % of the incoming waves and the mean wave overtopping discharge q per meter dike crest length:

$$R_{u2\%} = 1.65 \cdot \gamma_\beta \cdot \gamma_b \cdot \gamma_r \cdot \xi_{m-1,0} \cdot H_{m0} \quad (1)$$

$$\text{with its maximum: } R_{u2\%} = \gamma_\beta \cdot \gamma_r \cdot \left(4.0 - \frac{1.5}{\sqrt{\xi_{m-1,0}}} \right) \cdot H_{m0} \quad (2)$$

$$\frac{q}{\sqrt{g \cdot H_{m0}^3}} = \frac{0.067}{\sqrt{\tan \alpha}} \cdot \gamma_b \cdot \xi_{m-1,0} \cdot \exp \left(-4.75 \frac{R_c}{\xi_{m-1,0} \cdot H_{m0} \cdot \gamma_b \cdot \gamma_f \cdot \gamma_\beta \cdot \gamma_v} \right) \quad (3)$$

$$\text{with its maximum: } \frac{q}{\sqrt{g \cdot H_{m0}^3}} = 0.2 \cdot \exp \left(-2.6 \frac{R_c}{H_{m0} \cdot \gamma_f \cdot \gamma_\beta} \right) \quad (4)$$

based on the breaker parameter $\xi_{m-1,0}$ (also known as Iribarren number and surf similarity parameter):

$$\xi_{m-1,0} = \frac{\tan \alpha}{\sqrt{H_{m0}/L}} \quad (5)$$

with wave length L , wave height H_{m0} , crest freeboard height R_c , the gravity acceleration g and the angle of dike slope α . The influence of dike characteristics is taken into account by using influence factors γ like γ_b in case of a berm, γ_f describing slope roughness and γ_c in case of a crest wall. The influence of oblique wave attack on wave run-up and wave overtopping is considered with the influence factor γ_β . Several former investigations aimed at quantifying the influence of oblique wave approach. The elaborated formulas are summarized in the following:

$$\begin{aligned} \gamma_\beta &= 1.0 & 0^\circ \leq \beta < 10^\circ \\ \gamma_\beta &= \cos^2(\beta - 10^\circ) & 10^\circ \leq \beta \leq 50^\circ \\ \gamma_\beta &= 0.6 & 50^\circ < \beta \leq 80^\circ \end{aligned} \quad \begin{array}{l} \text{(van der Meer, 2010,} \\ \text{de Waal \& van der Meer, 1992)} \end{array} \quad (6)$$

$$\begin{aligned} \gamma_\beta &= 0.6 - 0.02 \cdot (\beta - 80) & 80^\circ < \beta \leq 110^\circ \\ \gamma_\beta &= 1 + 0.0095 \cdot \beta & \end{aligned} \quad \begin{array}{l} \text{(Murphy et al., 2001)} \end{array} \quad (7)$$

$$\begin{aligned} \gamma_\beta &= 0.10 + 0.90 \cdot \cos\beta \quad (1:3 \text{ sloped dike}) \\ \gamma_\beta &= 0.35 + 0.65 \cdot \cos\beta \quad (1:6 \text{ sloped dike}) \end{aligned} \quad \begin{array}{l} \text{(Oumeraci et a., 2002)} \end{array} \quad (8)$$

$$\gamma_\beta = 1.0 - 0.0076 \cdot \beta \quad \begin{array}{l} \text{(Kortenhaus et a., 2006)} \end{array} \quad (9)$$

$$\begin{aligned} \gamma_\beta &= 0.39 + 0.61 \cdot \cos^2 \beta \quad (1:3 \text{ sloped dike}) \\ \gamma_\beta &= 0.51 + 0.49 \cdot \cos^2 \beta \quad (1:6 \text{ sloped dike}) \end{aligned} \quad \begin{array}{l} \text{(FlowDike, 2012)} \end{array} \quad (10)$$

The formula for a 1:6 sloped dike by Oumeraci et al., 2002 is similar to Wagner & Bürger, 1973 for steeper dike slopes. The formulae are plotted in Figure 11 together with measurement results and show how the influence factor γ_β depends on the angle of wave attack β . An angle of wave attack $\beta = 0^\circ$ describes a perpendicular wave approach. To take into account the different investigated sea states the graphs are marked with different colours.

For smaller angles of wave approach the majority of the curves are similar. The shapes of the different curves are very dissimilar for $\beta > 30^\circ$ and there is only one proposed formula considering very oblique wave approach with angles of wave attack $\beta > 80^\circ$. Multidirectional sea states lead to at least slightly lower overtopping discharges than unidirectional sea states. The difference may lie in the range of scattering.

Overall, investigations are required to analyse the influence of very oblique and slightly offshore waves ($\beta > 90^\circ$) and a corner in the dike line. Therefore, the CornerDike project was originated to develop and enhance the design guidance for sea dikes.

3. MODEL SET-UP

The model tests were performed in the shallow water basin of the Danish Hydraulic Institute (DHI) in Hørsholm, Denmark. This 35 m long and 25 m wide basin with an overall depth of 0.8 m can be used for combined wave and current tests as they have been carried out by this user group within two HYDRALAB-III-projects before (cf. FlowDike, 2012, Bornschein & Pohl, 2012, Bornschein et al., 2012, Krüger et al., 2012). The general model layout in plan is given in Figure 1. A segmented wave generator was installed along one longer side of the basin. The investigated dike was built up opposite the wave maker.

For the CornerDike project, the 18 m long wave generator has been extended on its left side (in direction of the waves) by a 4 m long portable wave generator. The 44 segments of this combined wave generator had a width of 0.5 m and a height of 1.2 m each and could be used to generate multidirectional waves.

The dike was built up in the left part of the basin with a seaward slope of 1:4, which is typical for river and coastal dikes. The dike consisted of three parts (see Figure 1). The inner angle between the P-dike line and the wave generator was 15° . The N-dike was situated rectangular with respect to the P-dike. A convexly shaped quarter cone formed the connection between these both parts. This model set-up allowed an investigation of a very wide range of angles of wave attack between 0° and 112.5° . An overview of the dike structure and lengths of its different parts is shown in Figure 1.

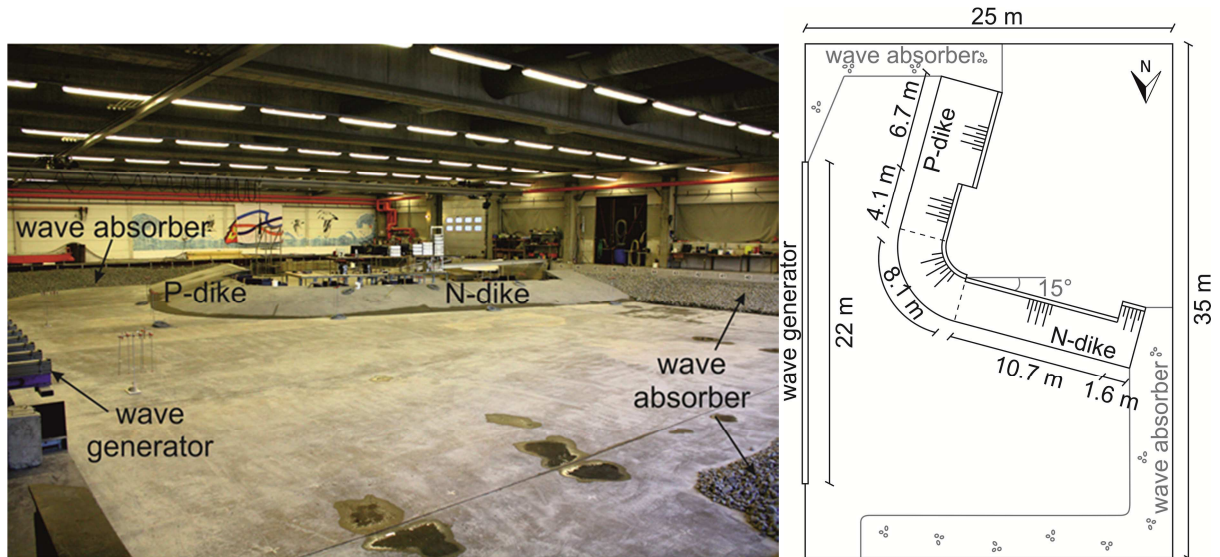


Figure 1: Overview of the model set-up (left) and plan view (right).

As the presumed overtopping discharges were considerably higher for the P-dike than for the N-dike, different crest heights were adjusted at the P-dike (0.75 m) and at the N-dike (0.7 m). That part of the dike which was not considered during the overtopping tests had a crest height of 1.0 m. This was in preparation for run-up tests which required a higher dike. Stone rip-rap was used in the rear and on the sides of the basin as a wave absorber to mitigate wave reflection and diffraction. Therefore, coarse gravel was placed along the vertical walls of the basin (cf. Figure 2).



Figure 2: Wave absorber in the southern part of the basin (left) and the northern part (right).

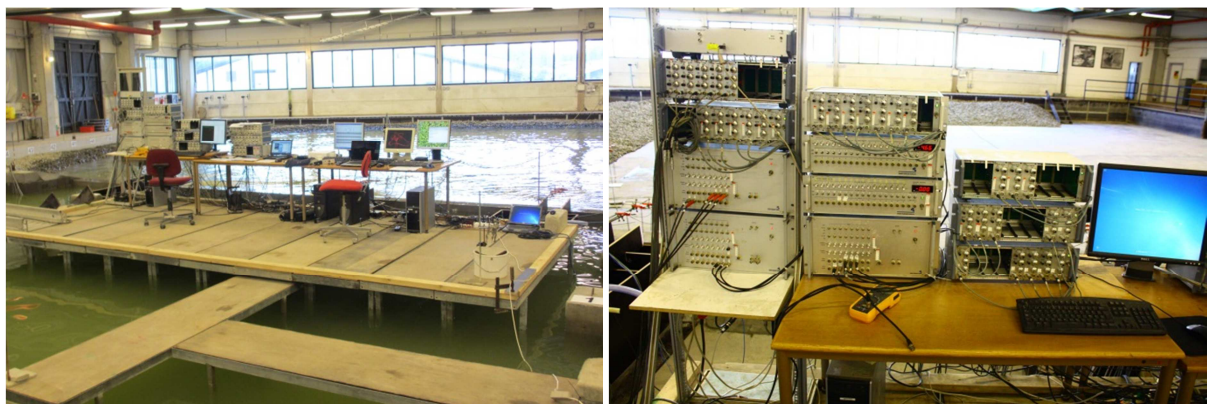


Figure 3: Platform (left) and data acquisition devices (right).

Before flooding the basin, the whole additional equipment such as data acquisition, amplifiers and computers were set up on an elevated platform in the centre of the basin to avoid them getting wet. Figure 3 shows the platform (left) and parts of the data acquisition devices (right). A constant water level and temperature were hold during the tests.

Wave overtopping was investigated in a first test series. Therefore the dike itself was only made up by the seaward slope and the dike crest. The landward slope was omitted. A seaward brick supported the seaward slope out compacted gravel. The whole structure was finished with render. Five overtopping units (OU 1 to OU5) were used for measurements of overtopping volume and situated at the landward side of the dike. Two units were built up behind the P-dike and three behind the N-dike (cf. Figure 4). Due to the positioning of overtopping units along the N-dike, it was possible to investigate the development of overtopping discharges along the dike line.

All overtopping units were made of plywood and were constructed identically (see Figure 5) except for different overflow channel widths at the P-dike and N-dike. As the presumed mean overtopping discharges were higher for the P-dike than for the N-dike, the overflow channels at the P-dike were narrower (0.1 m) as at the N-dike (0.3 m) to adjust the overtopping volumes. The gap between each overflow channel and the dike crest was filled up with silicone to smooth the junction and to avoid any water losses.



Figure 4: Numeration and position of overtopping units.

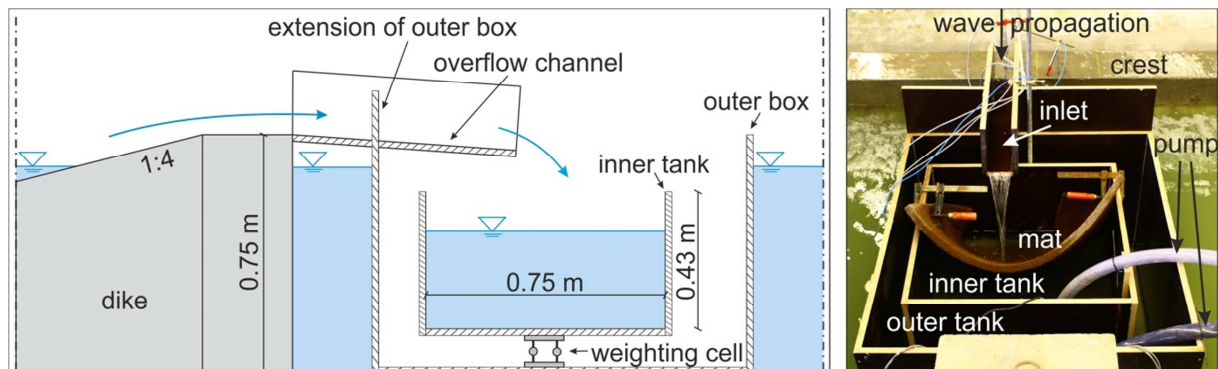


Figure 5: Cross-section of one overtopping unit at the P-dike (left) and overtopping unit at P-dike seen from the landward side of the dike (right).

Figure 5 shows a cross section of an overtopping unit at the P-dike. Overtopping water flows over an overflow channel into the inner tank (0.75 m x 0.75 m x 0.43 m). In this inner tank, the weight of overtopping water is measured by a 0.1 m high weighting cell that was fixed beneath the inner tank. The outer box contained the weighting cell and the inner tank. This way, the weighting cell and inner tank were positioned in a dry area and prevented from being lifted up. The wall of the outer box next to the dike was extended to avoid water splashing into the inner tank. Additionally, a mat was placed in the overtopping tank to reduce the noise of the signals caused by the inflow of water and impact on the bottom of the inner tank. Standard pumps were installed in the inner tanks (see Figure 5 right). They were used to empty the inner tanks during and after the tests as the overtopping boxes were not big enough to collect the whole amount of overtopped water of each test. Furthermore, pumps were used in the outer boxes to keep the water level in these boxes as low as possible in the case that there was a leak.

Flow velocity and flow depth on the dike crest are investigated using the signals of 15 small wave gauges, two mini propellers and four micro propellers that were installed on the 0.28 m wide dike crest and on the dike slope. Mini and micro propellers were used to record overtopping flow velocities. For this purpose two MiniWater6 Mini and four MiniWater6 Micro propellers by Schiltknecht,

Switzerland were installed on the dike crest. All propellers were calibrated before the tests. Three small wave gauges (0.25 m high) were installed in front of each overtopping unit on the dike slope and dike crest (seawards and landwards). The wave gauges were placed in-line and centred in front of the inlet channels. The mini and micro propellers were installed 0.20 m to the left (P-dike) or to the right (N-dike) of the wave gauges.

A second test series was focused on wave run-up. The still water level (SWL) was set to 0.70 m for all wave run-up tests. The overtopping units were demounted and a run-up board was attached to the top of the dike to enlarge the possible wave run-up area (cf. Figure 6).



Figure 6: Model set-up with run-up boards and gauge scale at the P-dike (left) and at the N-dike (right).

To analyse the wave run-up height two independent systems were used – capacitive gauges and video cameras (cf. Figure 8). The two capacitive gauges (CG1 and CG2) were installed near the dike corner. One was installed on the P-dike and one on the N-dike. Five cameras (C1 to C5) were positioned in front of the dike line. One camera (C1) recorded wave run-up at the P-dike, another at the cone (C2) and three additional cameras were installed along the N-dike (C3 to C5). The latter were mounted on the indoor crane. Cameras C1 and C2 were attached to two different support frames which were positioned inside the shallow wave basin.

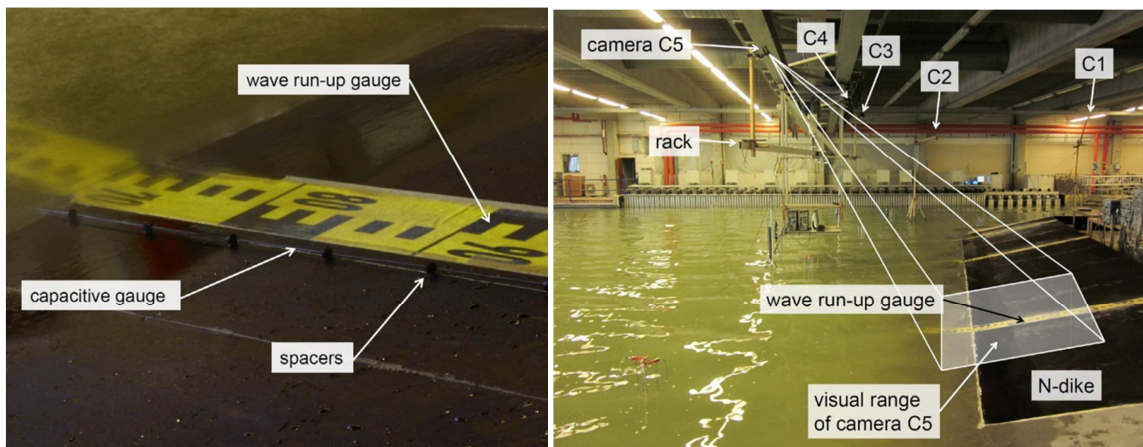


Figure 7: Capacitive and run-up reference scale (left) and position of the cameras (right).

Adhesive tape with a gauge scale was added to the run-up board as reference for video recording (see Figure 6 and Figure 7). Frame rate and camera resolution for all used cameras are summarized in Table 1.

Both, unidirectional (long-crested) and two types of multidirectional (short-crested) waves were applied during the tests using a JONSWAP spectrum. Test with long-crested waves provided data to evaluate the reliability of the model set-up and for comparison with results to former investigations (eg. FlowDike, 2012).

Table 1: Overview of used cameras for wave run-up recording.

camera	position	name	Camera resolution [pixel]	Frame rate [frames/s]
C1	P-dike	VRmagic VRmC-3+BW-PRO	754 x 480	13
C2	Cone	VRmagic VRmC-3+PRO	750 x 476	29
C3	N-dike	Sanyo VPC-FH1	1920 x 1080	25
C4		Sony HDR-XR200VE	1920 x 1080	29
C5		Sony DCR-SR55	1024 x 576	25

Table 2: Summary of test configuration.

dike slope	1:4					
crest height [m]	wave overtopping tests: P-dike: 0.75; N-dike: 0.70 wave run-up tests: 1,20					
water level [m]	0.60, 0.65, 0.68, 0.70					
freeboard height R_c [m]	P-dike: 0.15, 0.10, 0.07 N-dike: 0.10, 0.05, 0.02					
wave crestedness σ [°]	long-crested waves: $\sigma = 0^\circ$ ("long ref") short-crested waves: $\sigma = 34^\circ$ ("short 1") and $\sigma = 12^\circ$ ("short 2")					
wave height H_s [m]	0.07	0.07	0.10	0.10	0.15	0.15
and wave period T_p [s]	1.339	0.947	1.601	1.132	1.960	1.386
angle of wave approach β [°]	7.5, 15, 22.5, 30, 37.5, 45, 52.5, 60, 67.5, 75, 90, 97.5, 105, 112.5					

During the CornerDike project, the wave field was measured at seven positions (see Figure 8). Wave arrays (WA) consisting of three or five wave gauges (WA1 to WA7) and one-point-measurements (OPM1 to OPM4) containing one wave gauge and one ADV were used.

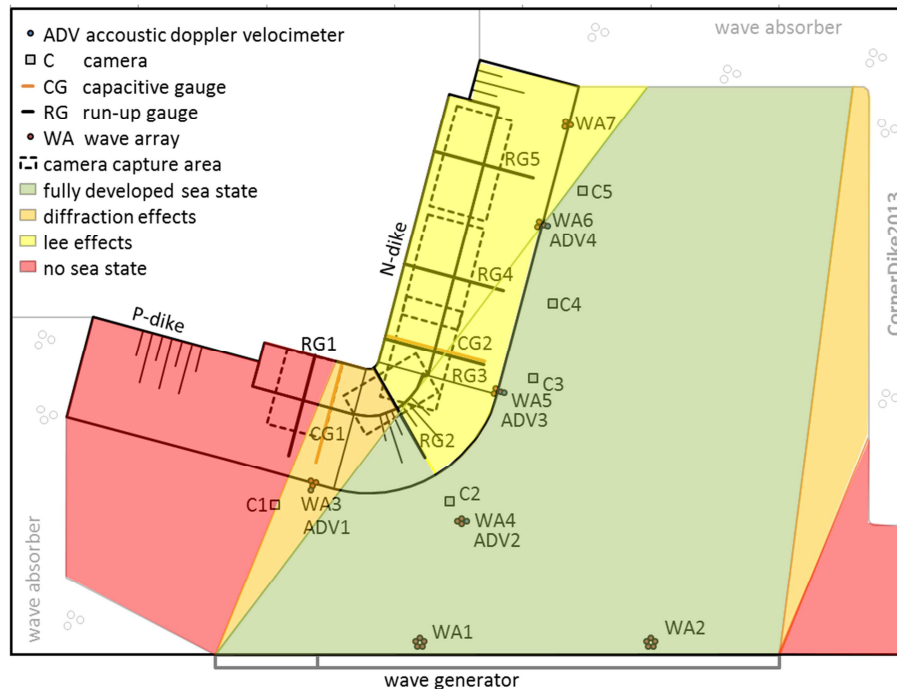


Figure 8: Shallow water basin with experimental set-up and positions of the measurement devices for wave run-up and wave characteristics (reliability analysis for p225, see Table 4).

Large wave gauges (0.5 m and 0.6 m high) were used for the one-point-measurement as well as for the wave arrays. Water level oscillations cause a change of conductivity between the two thin steel electrodes of the wave gauges that is measured and converted into the corresponding water surface elevation. The one-point-measurements (OPM) measured the water surface elevation and the direction of the waves in x and y direction so that the directional spectrum of the wave field could be analysed.

3. DATA ANALYSIS AND FIRST RESULTS

Models of structures and natural processes are often connected with simplifications and restrictions. These influences are known as model and scale effects and have to be considered during the analyses. One aspect of imperfect replications within the CornerDike project was the limited width of the generated wave field due to the finite length of the wave generator. Consequently, some areas of the basin lay, depending on the direction of the generated wave field, within an area outside of the fully developed sea state (see red areas in Figure 8). At the boundary of the generated wave field wave diffraction might have an influence on the wave characteristics. Data from measuring instruments (e.g. wave run-up gauges or wave overtopping units) that were positioned in these areas have to be used with caution or have to be omitted during analyses.

The results of a reliability analysis of the measured overtopping volume and recorded wave run-up heights are summarised in Table 3 and Table 4.

Table 3: Reliability of measured overtopping volume (position of the measurement device was ■ = within fully developed wave field; ■ = prone to diffraction effects, ■ = prone to lee effects; ■ = outside of fully developed wave field).

Test series	P-Dike			N-Dike			
	$\beta_{P-Dike} [^\circ]$	OU 1	OU 2	$\beta_{N-Dike} [^\circ]$	OU 3	OU 4	OU 5
m300	45	■	■	45	■	■	■
m150	30	■	■	60	■	■	■
p0	15	■	■	75	■	■	■
p075	7,5	■	■	82,5	■	■	■
p150	0	■	■	90	■	■	■
p225	7,5	■	■	97,5	■	■	■
p300	15	■	■	105	■	■	■
p375	22,5	■	■	112,5	■	■	■

Table 4: Reliability of film recorded run-up (position of the measurement device was ■ = within fully developed wave field; ■ = prone to diffraction effects, ■ = prone to lee effects; ■ = outside of fully developed wave field).

Test series	P-Dike										Corner		N-Dike																															
	$\beta_{P-Dike} [^\circ]$	Camera 1 (T265-T294)*										$\beta_{Cone} [^\circ]$	Camera 2	$\beta_{N-Dike} [^\circ]$	Camera 3										Camera 4										Camera 5									
		1	2	3	4	5	6	7	8	9	10				1	2	3	4	5	6	7	8	9	10	1	2	3	4	5	6	7	8	9	10	1	2	3	4	5	6	7	8	9	10
m300	45	■										0	■	45	■										■										■									
m150	30	■										15	■	60	■										■										■									
p0	15	■	■									30	■	75	■										■										■									
p150	0	■	■									45	■	90	■										■										■									
p225	7,5	■										52,5	■	97,5	■										■										■									
p300	15	■										60	■	105	■										■										■									
p375	22,5	■										67,5	■	112,5	■										■										■									

The run-up height $R_{u,2\%}$ were obtained by image data processing using a MATLAB procedure similar to the video analysis in the FlowDike-project (see Bornschein & Pohl, 2012). The video analysis and also the reliability analysis were conducted for 10 vertical stripes within the capture area of each camera 1, 3, 4 and 5 (see Figure 8 and Table 4). Only one vertical stripe within the capture area of camera 2 was considered which was equal to the central portion of the cone.

In the first step a wave field analysis was carried out based on measured wave heights. The wave field development and consequently also wave run-up and overtopping processes are influenced by many effects such as wave breaking, diffraction and refraction. Observations during the model tests showed a general pattern of the wave evolution along the dike: Waves are redirected around the corner, then interact with approaching waves and finally slide along the straight-aligned dike leg in the form of wave rollers. The development of the wave height and positions of wave energy concentrations depend on the wave direction and wave parameters.

To allow a comparison with numerical results, a simulation with the software SWAN was made considering three different test conditions regarding generated wave direction. The results of the numerical simulations reproduced well the wave height distribution which was observed in the model set-up. A maximum wave height was observed at the cone due to accumulation of wave energy at the convex shaped dike line. Along the straight-aligned dike leg, the wave height decreased more or less continuously with increasing distance from the corner.

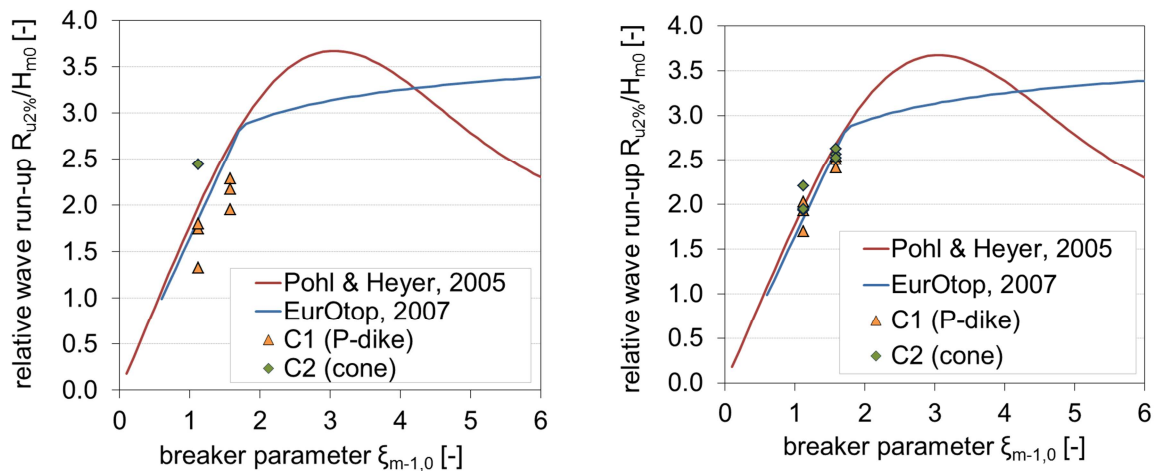


Figure 9: Measured relative wave run-up height for reference tests with long crested waves (left) and short crested waves (right) in comparison to known formulae (right).

In a second step, reference values of wave run-up and wave overtopping for perpendicular wave attack with $\beta = 0^\circ$ have been determined. All reference values for wave run-up regarding tests with long and short crested waves are presented in Figure 9. In addition known formulae by Pohl & Heyer, 2005 and EurOtop, 2007 plotted. As expected camera 2 at the cone observed higher values of relative wave run-up due to accumulation of wave energy at the convex shaped dike line. The results of reference tests for camera 1 (P-dike) are influenced by diffraction effects at the boundary of the generated wave field. As anticipated the wave field is more influenced by these diffraction effects in case of long crested waves than in case of short crested waves.

Overall there is a good agreement between measured and predicted values. For wave run-up a maximum difference of 12 % was calculated. The measured values of wave overtopping and the predicted values using the formula by EurOtop, 2007 showed a maximum difference of 15 %.

In a third step all influence factors were calculated by putting the measured values of an investigated angle in relation to the results of the tests with perpendicular wave approach. Influence factors have been derived from test data of waves with an angle of wave attack of $0^\circ < \beta \leq 112.5^\circ$. The higher values correspond to very oblique and slightly offshore waves. Even in case of investigated offshore waves a very small but still existing wave run-up and wave overtopping was observed. The results show that further investigations with angles of wave approach of $\beta > 112.5^\circ$ are required.

All results for tests with long-crested waves are presented in Figure 10. The figure includes empirical formulae for long-crested waves as presented in section 2 (equation 6 to 10) and two theoretically derived functions (Bornschein & Pohl, 2012) as boundary values. Results for $\beta \leq 45^\circ$ were obtained at the P-dike and data for $\beta \geq 45^\circ$ were found at the N-dike. An in depth analysis and the derivation of prediction formulae are currently under work.

Measurement results for wave run-up were compared to the Czech standard 75 0255 (Spano, 2014). The findings considering wave run-up heights with a probability of exceedance of 1 % are similar to the findings stated above.

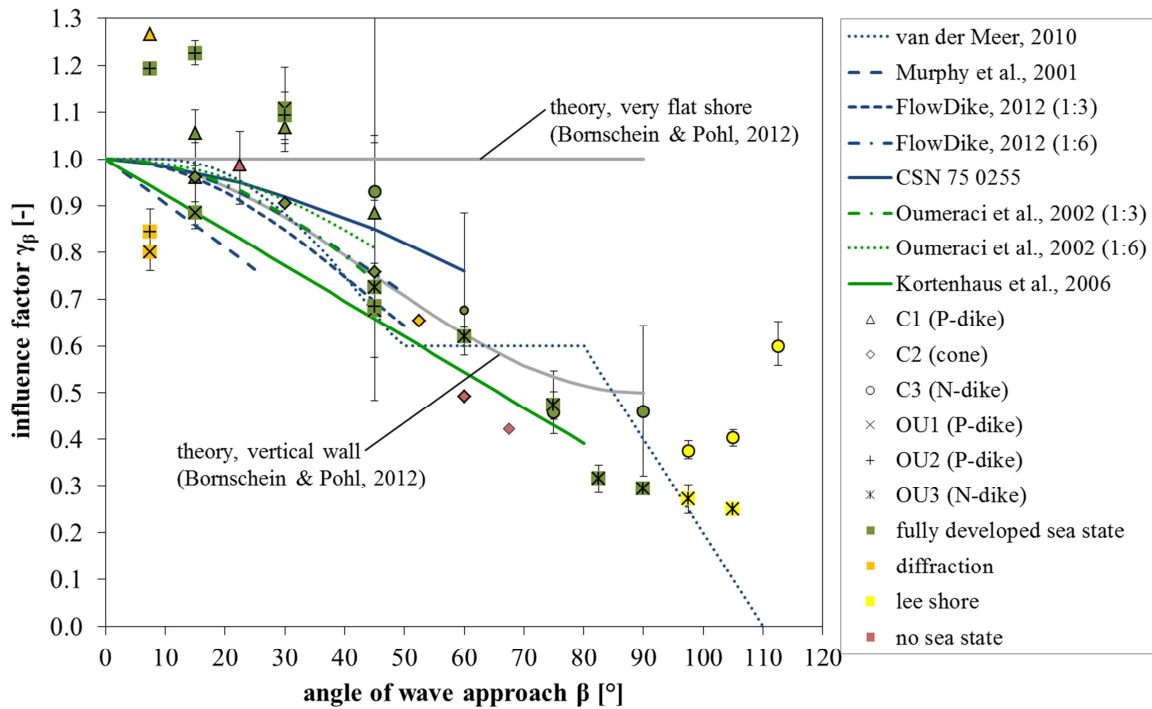


Figure 10: Influence of oblique wave approach on wave run-up and wave overtopping: available empirical formulae for influence factor γ_β (blue lines – long-crested waves, green lines – long and short-crested waves) together with data from CornerDike tests with long-crested waves.

Result analysis for short-crested waves is currently under work. Until now the data show a significant lower influence of very oblique wave attack on wave run-up and wave overtopping which is equal to higher values of the influence factor γ_β for $\beta > 45^\circ$. Overall the influence factor γ_β regarding wave run-up are slightly higher than the influence factors considering wave overtopping which is consistent with results of tests with long-crested waves.

ACKNOWLEDGEMENT

This work has been supported by European Community's Seventh Framework Programme through the grant to the budget of the Integrating Activity HYDRALAB IV within the Transnational Access Activities, Contract no. 261520. The authors wish to express their thanks to the EU for funding and to the DHI as well as to the project partners, Prof. Schüttrumpf, Dr. J. v. d. Meer, Prof. J. Riha and further colleagues from these institutions for the excellent cooperation.

REFERENCES

Bornschein A. and Pohl, R. 2012. Wave run-up of breaking and non-breaking waves, *The Coastlab 12 Book of Proceedings, COASTLAB, Gent*, pp. 333-342

ČSN 1985. Calculation of wave impact on water reservoir and backwater structures, Czech standard 75 0255 (in Czech)

EAK 2002. Empfehlungen für die Ausführung von Küstenschutzwerken durch den Ausschuss für Küstenschutzwerke, *Kuratorium für Forschung im Küsteningenieurwesen, Heft 65, Westholsteinische Verlagsanstalt Boyens & Co, Heide in Holstein*, corrected version 2007.

EurOtop 2007. Wave Overtopping of Sea Defences and related Structures – EurOtop Manual, *Die Küste*, issue 73, ISBN 978-3-8042_1064-6.

FlowDike 2012. Influence of wind and current on wave run-up and wave overtopping (FlowDike), *Final Report, RWTH Aachen and TU Dresden, Germany*.

Heyer T. and Pohl R. 2005. Der Auflauf unregelmäßiger Wellen im Übergangsbereich zwischen branden und Schwingen, *Wasser und Abfall, Vol. 5*, pp. 34-38.

Kortenhaus, A., Geeraerts, J., Hassan, R. 2006. Wave run-up and overtopping of sea dikes with and without stilling wave basin under 3D wave attack (DIKE-3D), *Final Report, Braunschweig, Germany*.

- Krüger, N., Bornschein, A., Pohl, R. 2012. Wellenaufschlag an Deichen unter komplexen Randbedingungen, *Wasserwirtschaft, issue 12, pp. 15-19*
- Lorke, S., Pohl, R., Schüttrumpf, H. 2012. Wellenüberlauf an Flussdeichen, *Wasserwirtschaft, issue 12, pp. 15-19*
- Oumeraci H., Möller J., Schüttrumpf, H., Zimmermann C., Daemrich K.-F., Ohle N. 2002. Schräger Wellenaufschlag an Seedeichen. *Final Report, BMBF research project KIS 015/016. LWI Report No. 881 / FI Report No. 643/V. Braunschweig, Germany.*
- Scheres, B. 2013. Effect of very oblique waves on wave overtopping, *Master Thesis, Institute of Hydraulic Engineering and Water Resources Management, RWTH Aachen*
- Spano, M. 2014. Data analysis CornerDike-project, *internal report, Brno University of Technology*
- de Waal, J.P. and van der Meer, J.W. 1992. Wave run-up and overtopping on coastal structures, *Proceedings 23th International Conference on Coastal Engineering, Venice, Italy, pp. 1758-1771.*
- van der Meer, J.W. 2010. Influence of wind and current on wave run-up and wave overtopping – detailed analysis on the influence of current on wave overtopping, *HYDRALAB III, project FlowDike, 12th May 2010.*
- Wagner H. and Bürger W. 1973. Kennwerte zur Seedeichbemessung, *Wasserwirtschaft Wassertechnik. Vol. 23, Issue 6, Berlin, Germany, pp. 204-207.*
- Wolf, V. 2013. Schräger und gerader Wellenaufschlag an speziellen Deichformen, *Diplomarbeit, Institut of Water Engineering and Applied Hydromechanics, TU Dresden*